International Journal of Pharmaceutics 672 (2025) 125283

Contents lists available at ScienceDirect

International Journal of Pharmaceutics

journal homepage: www.elsevier.com/locate/ijpharm

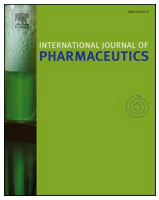

Curcumin-laden hydrogel coating medical device for periprosthetic joint infection prevention and control

Nina Burduja [a,b,1], Nicola F. Virzì [c,1], Giuseppe Nocito [a], Giovanna Ginestra [b], Maria G. Saita [d], Fabiola Spitaleri [d], Salvatore Patanè [e], Antonia Nostro [b], Valeria Pittalà [c,*], Antonino Mazzaglia [a,*]

[a] National Research Council, Institute of Nanostructured Materials (CNR-ISMN) URT of Messina at Dept. of Chemical, Biological, Pharmaceutical and Environmental Sciences (ChiBioFarAm), University of Messina, Viale Ferdinando Stagno d'Alcontres, 31 98166 Messina, Italy
[b] Department of Chemical, Biological, Pharmaceutical and Environmental Sciences (ChiBioFarAm), University of Messina, Viale Ferdinando Stagno d'Alcontres, 31 98166 Messina, Italy
[c] Department of Drug and Health Science, University of Catania, Viale Andrea Doria 6 95125 Catania, Italy
[d] Medivis, Via Carnazza 34/C 95030 Tremestieri Etneo, Italy
[e] Department of Mathematical and Computer Sciences, Physical Sciences and Earth Sciences (MIFT), University of Messina, Viale Ferdinando Stagno d'Alcontres, 31 98166 Messina, Italy

ARTICLE INFO

Keywords:
Curcumin
Vancomycin
DAC
Hyaluronic acid
Polylactic acid
aPDT
Hydrogel
Periprosthetic Joint Infection
MRSA
Antibacterial Coating

ABSTRACT

The Periprosthetic Joint Infection (PJI) is one of the most important complications of the joint arthroplasty. This surgical procedure is rising worldwide and is further affecting the public health because of the widespread resistance to antibiotics. New therapeutic strategies and innovative antimicrobial biomaterials development are needed to eradicate pathogens without inducing resistance and accelerating recovery. In this direction, herein Curcumin I- (Cur-) loaded DAC® (Defensive Antibacterial Coating, a hydrogel based on hyaluronic acid conjugated to polylactic acid, hereafter named DAC) has been built on. To incorporate Cur in the DAC, thus obtaining Cur-DAC (Cur ≅ 0.93 mg/g), the generally recognized as safe (GRAS) propylene glycol (PG) was used as cosolvent. The drugs combinations of Cur (≅ 0.93 mg/g) and Vancomycin (Van) (at low dose that is ≅ 0.033 mg/g) within the hydrogel (Cur/Van-DAC) was alsoexperienced . Hydrogels were prepared and characterized by rheological investigations and their erosion together with the drug release profile over the time evaluated in physiological conditions. The nanohydrogels produced upon water dilution were characterized by AFM, DLS, and UV/Vis absorption and emission spectroscopies. Superior Cur stability over pH-, solvent- and photoinduced degradations resulted in the DAC matrix. The photoinduced antimicrobial activity of Cur-DAC against methicillin-resistant *Staphylococcus aureus* (MRSA) and vancomycin-resistant *Enterococcus faecium* was evaluated by spreading loaded DAC-based hydrogel onto titanium disk mimicking prosthesis, thus detecting a good reduction of bacterial load after 30 min of exposure to light and a subsequent decrease of cells number at 24 h in the absence of nutrients. The drug association in Cur/Van-DAC demonstrated the best activity against MRSA, even in the presence of nutrients, with respect to established DAC loaded with high amounts of Van (ranging from 18.7 mg/g to 45.8 mg/g) used during the surgery, due to the photoantibacterial activity of Cur, becoming promising to prevent and control joint infections.

1. Introduction

Due to higher life expectancy and to the increased expectations of mobility in older age, the number of joint arthroplasties is rapidly raising worldwide. Still nowadays different complications afflict this surgical operation, and Periprosthetic Joint Infection (PJI) is one of the most difficult to manage for both the patient and the treating centre (Spichler-Moffarah et al., 2023). When missed or undertreated, PJI leads to persistence of infection and multiple surgical revisions, leading to a long-term patient hospitalization, poor function, or disability or even

* Corresponding authors.
E-mail addresses: valeria.pittala@unict.it (V. Pittalà), antonino.mazzaglia@cnr.it (A. Mazzaglia).
[1] These authors contribute equally to this work.

https://doi.org/10.1016/j.ijpharm.2025.125283
Received 9 December 2024; Received in revised form 24 January 2025; Accepted 25 January 2025
Available online 30 January 2025

death due to general sepsis. Hence, there is a strong recommendation to set up adequate antibacterial surfaces to prevent bacterial adhesion (Bingyun Li et al., 2020; Pemmada et al., 2023) and colonization of prosthesis (Kumar et al., 2021; Romano et al., 2015). The concept of "race for the surface" explains as host and bacterial cells, during the first hours after surgery, compete to colonize the implant surface, and the probability of attachment of host cells decreases when bacterial cells adhere firstly to the surface, and *vice versa* (Turner et al., 2025). *Staphylococcus aureus* as well as multidrug resistant (MDR) bacteria and extensively drug resistant (XDR) bacteria, are the most frequent causative agents of PJI (Partridge et al., 2018; Yin et al., 2019). For treating PJI, Vancomycin (Van), a potent antibiotic of the glycopeptides' family, is active against Gram-positive bacteria (Abbas et al., 2024). Unfortunately, Van may have serious side effects such as ototoxicity and nephrotoxicity and there have been also reports of vancomycin-resistant enterococci (VRE) (Ahmed and Baptiste, 2018).

In this scenario the use of curcuminoids and in particular Curcumin I (Cur) from *Curcuma longa* are beneficial thanks to anti-inflammatory, antitumoral, analgesic, and immunomodulatory properties, for its multifaceted antibacterial mechanism of action (Li et al., 2020; Zheng et al., 2020) and as potential antibiotic resistance breaker (Marini et al., 2018). In addition, Cur is a well-known photosensitizer (PS) in antimicrobial photodynamic therapy (aPDT) (Dias et al., 2020; Maldonado-Carmona et al., 2020). Generally, aPDT exploits a PS with physical and chemical properties capable to interact with bacterial cells and by irradiation with Vis/NIR light it produces reactive oxygen species (ROS) and/or singlet oxygen ($^1O_2$) for targeting and killing pathogen agents. The entrapment of PS in drug delivery systems avoids photodegradation and stabilizes the molecule in non-aggregated forms to increase photodynamic efficiency. In this direction Liu et al (Liu et al., 2018) proposed Cur up-conversion nanoparticles to efficiently eradicate drug resistant bacteria in PJI. However, Cur translation into clinical use has been prevented by extremely poor water solubility, low bioavailability, low physical and chemical stability, and extensive fist-pass metabolism (Racz et al., 2022; Salehi et al., 2019).

Fast resorbable *peri*-operative hydrogel coating for prosthesis attracted attention due to their huge potentiality to fasten post-surgery recovery by means of bleeding control, preventing adhesions and biofilm formation, and promotion of osteointegration upon prosthesis implantation (Uneputty et al., 2022). This approach may replace already marketed medical devices used for many years in joint arthroplasties, such as the antibiotic-loaded polymethylmethacrylate. Indeed, its non-biodegradability, scarce antibiofilm effect, and capacity to induce resistance is making it less elective for modern applications (Fraval et al., 2024; Naoum et al., 2024; Romano et al., 2015). Polysaccharides based-hydrogels are versatile and resorbable able to entrap PEG-solubilized Cur by providing antibacterial response for wound-healing applications (Sood et al., 2023). On the other hand, recent findings highlighted the ability of PVA hydrogel to coat titanium prosthesis to prevent bacterial colonization (Lei et al., 2024). In the present work an already marketed fast-resorbable hydrogel named DAC® (Defensive Antibacterial Coating, hereafter indicated with DAC) (Giammona et al., 2010) was selected. DAC is composed of hyaluronic acid grafted to polylactic acid (HA-PLA), a well-known biocompatible and biodegradable polymer mixture. HA-PLA hydrogel has already proved to prevent biofilm formation *in vitro* and *in vivo*, and the onset of PJI in a large number of patients (Drago et al., 2014; Pitarresi et al., 2013; Romano et al., 2016). The available market kit is composed of a prefilled syringe containing sterile DAC powder that is filled during surgery with a solution of sterile water eventually mixed with an opportune antibiotic depending on the surgeon's choice, often formulated in a concentration range between 20 to 50 mg/mL. A few minutes after the reconstitution, the hydrogel can be directly spread onto the implant, which is then inserted into the body according to normal surgical procedure (Franceschini et al., 2020). Previously reported data confirmed that the combination of natural compounds with antibiotics such as Cur and Van, could lead to a synergistic effect which can fight the antimicrobial resistance (Yadav et al., 2020). Even if the combination of Cur and Van into hydrogel systems (Huang et al., 2022b) and other formulations (Huang et al., 2022a) may be not totally new, the co-entrapment of natural compounds such as Cur and an antibiotic as Van in trade HA-PLA-based hydrogel represents a novel approach to improve the antibacterial properties of these medical device coatings, especially for photodynamic treatments.

Following our ongoing research on nanoformulations containing curcuminoids (Virzi et al., 2023; Zagami et al., 2023), here a new Cur-and its association with Van-loaded in DAC-based hydrogel formulations have been built on. We aimed to develop a formulation suitable for fast translation from the laboratory to the clinic. For this reason, the composition of the hydrogel was planned in order to use only generally recognized as safe (GRAS) materials, which can allow a fast-track approval while remaining within the medical device category. One of our primary objectives was to massively increase the Cur solubility into a fast resorbable and biofluid system as the DAC hydrogel, thus allowing that Cur can directly reach the periprosthetic site and increase its *in situ* bioavailability. Another aim was to potentiate the antibacterial action of DAC and at the same time to confer photoactivation thanks to antimicrobial photodynamic properties of the encapsulated Cur, immediately before implantation and to guarantee its sustained release in the periprosthetic site after implantation for the overall prevention of PJI. Finally, the combination of DAC and Cur in association with Van was tested to verify whether Cur reduces the antibiotic concentration, reducing the risk of Van-related side effects.

2. Material and methods

2.1. Materials

DAC® (Defensive Antibacterial Coating), a conjugate between Hyaluronic Acid and Poly-Lactic Acid (HA-PLA) [batch U90183, powder] was a generous gift from Novagenit S.r.l. (Mezzolombardo, Italy) (Giammona et al., 2010). Curcumin from *Curcuma longa* (Turmeric, CAS: 458–37-7, > 65 % from HPLC), dichloromethane (DCM) (ACS reagent, ≥ 99.9 % from GC), acetone (ACS reagent > 99.5 %), dimethyl sulfoxide (DMSO) (ACS reagent, ≥ 99.9 %), propylene glycol (PG) (> 99 % from GC), vancomycin hydrochloride (Van) were purchased from Merck-Sigma Aldrich (Darmstadt, Germany). Water for injectable use (ultrapure water) was purchased from S.A.L.F. (S.A.L.F. S.p.A. Laboratorio Farmacologico, Cenate Sotto, Italy). Sandblasted titanium specimens 25 mm in diameter with a thickness of 5 mm and with a roughness of 1.5–4.5 μm were used as supports to spread DAC derivatives. Curcumin from *Curcuma longa* (Turmeric) was purified to Curcumin I ((1E,6E)-1,7-bis(4-hydroxy-3-methoxyphenyl)hepta-1,6-diene-3,5-dione, Cur) by column chromatography and characterized by ^{1}H NMR (Fig. S1), ^{13}C NMR (Fig. S2) and FT-IR (Fig. S3). Details are reported in SI.

2.2. Hydrogels preparation

Cur-DAC was prepared as follows by using a standardized procedure (Romano et al., 2016): a 2.7 mM stock solution of Cur (MW = 368.38 g/mol) was prepared in DCM and dispensed into a glass vial (1.4 mg). The solvent was evaporated under nitrogen flow to achieve a thin film of Cur which was solubilized by means of predetermined volume of PG (400 μL or 414 mg) achieving a final percentage of PG in the final PG/H_2O volume ratio of 28.57 % (29.28 % w/w). Cuncurrently, the DAC powder (42 mg) was weighed to achieve a 3 % w/w ratio in the final hydrogel, subsequently placed into a sterile polyethylene terephthalate (PET) luer-lock syringe and wet with the Cur solution in PG. Then, another syringe was filled with 1 mL of ultrapure water used to hydrate the mixture (see Fig. 1). The two syringes were connected by means of a luer-lock connector and, by repeated transfers between the two syringes, the resulting hydrogel was homogenized, so mimiking the in-clinic preparation protocol of commercially used DAC system, achieving a

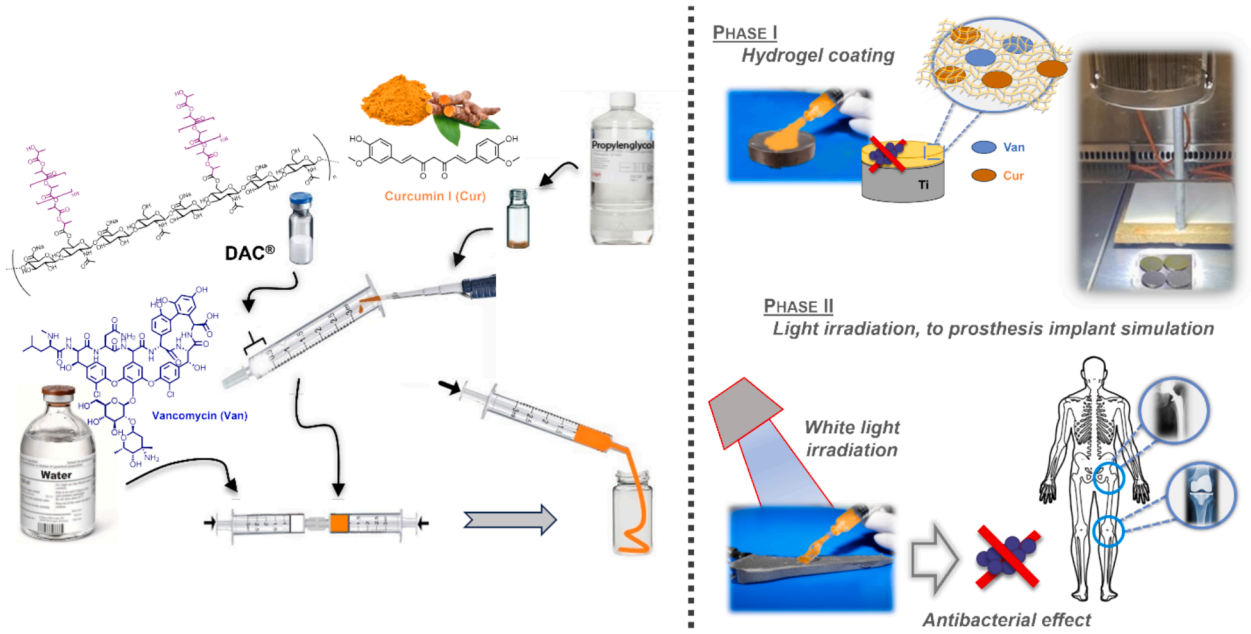

Fig. 1. Left: Sketched view of the preparation of DAC-based hydrogels. Right: Phases of the procedure simulating the preparation of antibacterial coating in the operating room for titanium-based prosthesis for hip and knee replacement: I) Extemporaneous preparation of the hydrogel and coating of the surface of a titanium disk mimicking an arthroprosthesis, II) Light irradiation (lamp irradiating disks at top right) and antibacterial effect evaluation.

theoretical concentration in the final hydrogel of 0.96 mg/g of Cur. Similarly, for the preparation of Cur/Van-DAC in a sterile PET syringe was poured the DAC powder (42 mg) which was then wet with the Cur solution in PG. Another syringe was filled with 1 mL of 27.6 μM Van (MW = 1449.25 g/mol) solution in ultrapure water prepared from the dilution of a previously prepared stock solution (400 μg/mL, 276 μM) (Fig. 1) and transferred, through the luer-lock connector, to wet the Cur-DAC in the other syringe by achieving the theoretical concentration in the final hydrogel of 0.96 mg/g and 0.0384 mg/g of Cur and Van, respectively (drug weight/hydrogel weight). As controls, Van-DAC and DAC samples (DAC and DAC 1 %), Van-DAC 0.5, Cur/Van-DAC 0.5, A, C and D (at different amount of DAC, Cur and Van see Table 1) were prepared by maintaining unaltered the PG/H_2O volume ratio.

2.3. Determination of drug content in the hydrogel

The actual Drug Loading (DL %), Theoretical Loading (TL %) and Entrapment Efficiency (EE %) were determined by Equations 1-3, respectively.

$$DL(\%) = \frac{measured\ amount\ of\ drug\ in\ hydrogel}{amount\ of\ hydrogel} \times 100 \quad (Eq.1)$$

$$TL(\%) = \frac{amount\ of\ drug\ initially\ added\ to\ formulation}{amount\ of\ hydrogel} \times 100 \quad (Eq.2)$$

$$EE(\%) = \frac{measured\ amount\ of\ drug\ in\ hydrogel}{amount\ of\ drug\ initially\ added\ to\ formulation} \times 100 \quad (Eq.3)$$

The amount of Cur (for the Equation 1 and 3) was estimated by solvent extraction method. Briefly, around 190 mg of freshly prepared Cur/Van-DAC and Cur-DAC hydrogels were diluted in 10 mL of ultrapure water and extracted several times with DCM until discoloration of the aqueous phase. The organic phase was collected, evaporated under reduced pressure, and solubilized with an exact volume of DCM to spectrophotometrically determine the concentration of Cur from a UV/Vis standard calibration curve (Zagami et al., 2023) in which the extinction coefficient (ε) at 419 nm in DCM is ≅ 47740 $M^{-1}cm^{-1}$. The drug loading was confirmed by the determination of the unloaded Cur extracted in DCM from the glassware used for the preparations.

The amount of Van was determined by High Performance Liquid

Table 1
Formulated DAC-based hydrogels.

Formulation[a]	Drug	Drug concentration (mg/g)[b]	DAC % (w/w)	Theoretical Loading (% ± SD)	Actual Drug Loading (% ± SD)	Entrapment Efficiency (% ± SD)
A	Cur	0.98	1	0.098 ± 0.001	–	–
Cur-DAC	Cur	0.96	3	0.096 ± 0.001	0.0932 ± 0.0001	97.1 ± 0.1
C	Cur	0.49	1	0.049 ± 0.001	–	–
D	Cur	0.48	3	0.048 ± 0.001	–	–
Cur/Van-DAC	Cur	0.96	3	0.096 ± 0.001	0.0932 ± 0.0001	97.1 ± 0.1
	Van	0.0384		0.004 ± 0.0005	0.003 ± 0.0005	86.97 ± 0.1
Van-DAC	Van	0.0384	3	0.004 ± 0.0005	0.003 ± 0.0005	86.97 ± 0.1
Van-DAC 0.5	Van	0.005	3	$4.35 \bullet 10^{-5}$	–	–
Cur/Van-DAC 0.5	Cur	0.96	3	0.096 ± 0.001	–	–
	Van	0.005		$4.35 \bullet 10^{-5}$	–	–
DAC	–	–	3	–	–	–
DAC 1 %	–	–	1	–	–	–

[a] All the formulations containing Cur were prepared by pre-dissolving Cur in PG/H_2O 29.28 % w/w.
[b] Drug weight/hydrogel weight (nominal concentrations initially used in the preparation of the hydrogel);[c]DAC weight (mg) in 100 mg of water.

Chromatography (HPLC). A Gemini® (Phenomenex Inc., Torrance CA-USA) 3 μm NX-C18 110 Å (150 mm x 4.6 mm) column equilibrated at 25 °C was used on Agilent 1200 (Agilent Technologies Inc., Santa Clara CA-USA) instrument setting the UV detector at 205 nm. The mobile phase was a gradient of methanol (MeOH) and H_2O/TFA (0.1 % v/v, TFA = trifluoroacetic acid), the solvents were HPLC gradient grade and degassed before the use. The elution method involved a flow rate of 1.0 mL/min and a gradient of 10 % MeOH 0–5 min, 27 % 5.5–10 min and 10 % 10.5–15 min with a post run of 5 min. The volume of the sample injected was 50 μL. Linearity of response was verified on Van solutions in ultrapure water by external calibration with analytical standards in the concentration range 0.05–2 μg/mL ($R^2 = 0.9998$, LOD = 0.03 μg/mL, LOQ = 0.05 μg/mL, analytical error ~ 5 %). The standard calibration curve, the chromatogram, and the HPLC method are reported in Fig. S4 and S5 and in Table S1. The Van loaded into Cur/Van-DAC and Van-DAC was estimated by the dilution of 50 mg of the hydrogel in 1 mL of MeOH/H_2O 1:1 v/v. Regarding the Van released from or within the nanohydrogel during the kinetic time-dependent hydrogel erosion studies, this was estimated dissolving in 500 μL of ultrapure water the freeze-dried samples collected during the analysis. The samples were then centrifuged for 20 min (5000 rpm, 5 °C) recovering the supernatant that was carefully transferred into HPLC vials. Samples were analyzed in triplicate.

2.4. Rheological investigations

Rheological measurements of hydrogels were conducted using a Bohlin CVO 100 rotational rheometer (Malvern Instruments Inc., Malvern UK) coupled with the Bohlin CVO 100 analysis software and employing parallel plate geometry (PP20) with a gap size of 1 mm and maintaining the temperature at 25 ± 2 °C with Bohlin Instruments Peltier module. Samples (Cur-DAC, Cur-Van/DAC, Van-DAC, DAC and DAC 1 %) were placed on the rheometer plate and allowed to equilibrate for 120 s before measurements. Experiments were conducted on freshly prepared samples and their viscoelastic properties were evaluated in terms of flow behavior (viscosity dependance on shear rate (γ) in the range of 0.03–1000 s^{-1}) as well as storage (G′), viscous (G″) and complex (G*) moduli using amplitude sweep experiments in strain control (strain range: 0.1–1000 %) at the constant angular frequency of 10 rad/s to determine the range in which the oscillatory tests can be carried out without destroying the sample structure, followed by the frequency sweep experiments to evaluate G′ and G″ magnitudes over a frequency range of 1–20 rad/s at a fixed strain 1 %. The inverted vial test was conducted on Cur-Van/DAC upon dilution ranging from final hydrogel produced (100 % w/w) to 12.5, 5 and 0.66 % w/w (hydrogel weight over water weight).

2.5. Morphological studies by Atomic Force Microscopy (AFM) and photoluminescence

The sample was obtained by spin coating a nanohydrogel dispersion (0.83 % w/w) onto a borosilicate glass surface previously cleaned with isopropanol. The morphology of the sample was studied using an AFM NT-MDT microscope (NT-MDT Spectrum Instruments Ltd., Limerick IE) equipped with a silicon tip (Ha_NC ETALON) suitable for high-resolution measurements. To measure the photoluminescence spectrum, the sample was excited using a 473 nm diode-pumped solid-state (DPSS) laser. The light produced by the sample was collected with a long working distance 100X objective and sent to a SOL MS3504i spectrometer (SOL Instruments GmbH, Augsburg DE) equipped with an Andor IDUS CCD (Andor-Oxford Instruments, Belfast UK). To cut off the laser light and improve the dynamics of the optical system, a Semrock RazorEdge (IDEX Health & Science LLC, West Henrietta NY-USA) optical filter was placed in the optical path before the spectrometer (Zagami et al., 2023).

2.6. Optical spectroscopy and Dynamic light scattering (DLS) characterization

UV/Vis absorption spectra were recorded on an HP/Agilent 8453 diode array spectrophotometer (Agilent Technologies Inc., Santa Clara CA-USA) and on a Jasco V-770 UV/Vis-NIR scanning spectrophotometer (Jasco Co, Tokio JP). Steady-state emission spectra were recorded with a Jasco FP-8550 (Jasco co., Tokyo JP). The samples were prepared by diluting in ultrapure water the produced hydrogels and placed in quartz cells (0.2 cm and 1 cm path length) at room temperature (25 °C) for the spectroscopic characterizations.

The average hydrodynamic diameter (D_H), width of distribution (polydispersity index, PDI) and ζ-potential of the diluted hydrogels (to 2.5 % w/w for samples A and C and to 0.83 % w/w for Cur-DAC, Cur/Van-DAC and Van-DAC and sample D in ultrapure water) were measured with a Malvern Zetasizer Nano ZS (Malvern Instruments Inc., Malvern UK), equipped with a He-Ne laser (λ = 633 nm, power = 4 mW). Each measurement was performed at an angle of 173° to the incident beam using the non-invasive backscattering technique (NIBS) at 25 ± 1 °C and recorded in triplicate. Deconvolution of the measured correlation curve into a dimensional intensity distribution was obtained using a non-negative least squares algorithm.

2.7. Colloidal stability and photostability of the nanohydrogel

The colloidal stability of DAC based nanohydrogels over the time was investigated by UV/Vis absorption spectroscopy and DLS technique upon dilution of the produced hydrogels in ultrapure water (2.5 % w/w for samples A and C and to 0.83 % w/w for Cur-DAC, Cur/Van-DAC, Van-DAC and sample D by setting DAC % w/w amount to 0.025 % w/w). Samples were freshly prepared, equilibrated for 15 min and analyzed at room temperature (R.T. ~ 25 °C) and then stored at 4 °C and 37 °C for their stability evaluation over the time (t = 0, 1, 3, 6 days). Each sample was produced and analyzed in triplicate.

The photostability of Cur was evaluated in different solvent/media such as DCM, PG and PG/H_2O (29.28 % w/w in PG), within Cur/Van-DAC and A nanohydrogels. Samples were irradiated under magnetic stirring in a quartz cell (1 cm path length, irradiation area 2 cm^2) using a white light-emitting diode (LED) (400 nm < λ_{em} < 700 nm, $\lambda_{em\ max}$ = 450 nm, 26000 lx, irradiance 3.81 mW/cm^2, Fluence 6.85 J/cm^2) that was also employed for photoinduced antibacterial activity assays. To minimize trivial effects on photodegradation rate calculations, the solutions of Cur were prepared to have around 10 % on absorbance difference at the emission maximum (450 nm) of the polychromatic light source. Cur/Van-DAC and A nanohydrogels were prepared respectively upon 0.83 % w/w and 2.5 % w/w hydrogel dilution in ultrapure water by setting DAC % w/w amount to 0.025 % w/w. The photostability was evaluated from the UV/Vis absorption spectra recorded over time intervals depending on the detected degradation rate of Cur until 90, 210 and 330 min for the DCM, PG and PG/H_2O solutions respectively and until 150 and 255 min for Cur/Van-DAC and A respectively. The reaction rate was calculated considering the intercept of the fitted linear plot of the early stage of the photoreactions and compared to the more photostable nanohydrogel A (Fig. 4c). Results were plotted as the absorbance differences over the initial absorbance as a function of the irradiation time.

2.8. In vitro release/erosion kinetics study

The erosion kinetics of Cur-DAC, Van-DAC and Cur/Van-DAC hydrogels were evaluated in 10 mM phosphate buffer saline (PBS), pH 7.4, 37 °C, and in time intervals between 30 min and 72 h. Cumulative drug release method was used for the purpose. 500 μL of PBS were added to the hydrogel (around 400 mg) to simulate the physiological environment inducing its erosion in form of nanohydrogel in which the drugs (Cur and Van) are dispersed. 100 μL of the dispersion were taken at

predetermined time (0.5, 1, 1.5, 2, 20, 24, 72 h) and replaced with 100 μL of fresh medium. The experiments were performed in triplicate and the results reported as mean value ± standard deviation (SD).

Due to the appreciable absorption of Cur in the visible region, its amount within the nanohydrogel was spectrophotometrically determined upon dilution to 1 mL in a 0.2 cm path length quartz cuvette, following the UV/Vis standard calibration curves which were previously determined and reported in Fig. S14. The calibration curves for the produced nanohydrogels were obtained from serial dilutions in ultrapure water of an initial amount of 50 mg of the hydrogels by plotting the extinction maximum values at 407 nm (or exceptionally at 412 nm only for the hydrogel C) vs the calculated concentration of Cur. For the all curves, the concentration of Cur was corrected for the encapsulation efficiency calculated for Cur-DAC and Cur/Van-DAC hydrogels. Extinction coefficients (ε) at 407 nm for Cur-DAC (~ 11350 $M^{-1}cm^{-1}$) and for Cur/Van-DAC (~ 10450 $M^{-1}cm^{-1}$) were used for the quantitative determinations.

HPLC was used to quantify the Van released from or within the nanohydrogel, the samples coming from the various time-dependent collection were freeze-dried for 24 h before the analysis (*vide supra on HPLC determination of Van*). The measurement results were converted into released percentage on the nanohydrogel normalizing for the effective amount of Cur (0.9325 mg/g) and Van (0.0334 mg/g) loaded into the hydrogel. To evaluate the kinetic profile of DAC-based hydrogels various mathematical models for drug release data fitting (Li and Mooney, 2016) were applied to including: first order, Higuchi, Korsmeyer-Peppas, Peppas-Sahlin and Hagen (Lu and Ten Hagen, 2020). Equations and evaluations are reported in Table S5 and from Fig. S17 to Fig. S20.

2.9. Antibacterial and photo-antibacterial activity

2.9.1. Minimal inhibitory concentration (MIC) and minimal bactericidal concentration (MBC)

The bacteria used in this study were *Staphylococcus aureus* ATCC 6538, methicillin resistant *S. aureus* (MRSA) ATCC 43300, vancomycin resistant *Enterococcus faecium* DSM 17050 (VRE-fm), *Escherichia coli* ATCC 10536, extended-spectrum β-lactamase (ESBLs)-producing *E. coli* DSM 105388, *Pseudomonas aeruginosa* ATCC 9027 and VIM-2 producing *P. aeruginosa* DSM102273. The samples assayed were as follows: Curcumin I in DMSO (Cur-DMSO) 20 mg/mL, Curcumin I in PG (Cur-PG) 2 mg/mL, Vancomycin in ultrapure water (Van), Cur-DAC (1/10 dilution in ultrapure water): 0.1 mg/mL (Cur) (correspondent to 0.096 mg/g (Cur) – 0.3 % w/w (DAC).

MIC and MBC were performed according to the guidelines of the Clinical and Laboratory Standards Institute (CLSI), C.L.S.I., 2020 with some modifications. Briefly, the samples were serially 2-fold-diluted in 96-well round-bottomed using Muller-Hinton Broth (MHB) and overnight bacterial cultures were inoculated to yield a final concentration of approximatively 5×10^5 colony-forming units (CFU)/mL. After incubation at 37 °C for 24 h, the MIC was considered the lowest concentration showing no bacterial growth. The MBC was determined by seeding 20 μL from all clear wells on Muller Hinton Agar (MHA) and incubated at 37 °C for 24–48 h. The MBC was defined as the lowest concentration that killed 99.9 % of the inoculum. The data from at least three replicates were evaluated and modal results were calculated. DMSO, PG, DAC and MHB were included as controls.

2.9.2. Photo-antibacterial activity of Cur-based systems

The antibacterial activity of Cur-PG (0.1 mg/mL) and Cur-DAC (1/10 dilution) after irradiation (30 min) was investigated against *S. aureus* (MRSA) ATCC 43300 and *P. aeruginosa* ATCC 9027. The overnight broth cultures grown in MHB were centrifuged at 3500 rpm for 15 min, washed with PBS and resuspended in order to obtain a final density of approximately 1–3 x 10^6 CFU/mL. The standardized bacterial suspension was inoculated into each well of a 96-well microplate containing the different nanohydrogels based on Cur. The microplate was irradiated for 30 min by white LED source irradiation (*vide the specimens in the 2.7 paragraph*) or kept in the dark. Afterwards, each sample was diluted in PBS, drop-plated in duplicate on MHA plate and incubated at 37 °C for 24–48 h. Later, colonies were counted at the most appropriate dilution and expressed as log CFU/mL. PG, DMSO and PBS were included as controls.

2.9.3. Antibacterial efficacy of DAC samples spread on titanium disks

Titanium disks (24 mm diameter) were dipped in 75 % ethanol for 60 min, washed and then sterilized at 121 °C. Each DAC hydrogel sample Cur/Van-DAC, Cur-DAC, Van-DAC, Cur/Van-DAC 0.5, Van-DAC 0.5 and DAC was spread on titanium disk to form a uniform coating on the metal surface. The exact amount of 50 ± 1 mg was determined using an analytical balance. The titanium disks were then aseptically placed at the bottom of each plate (33 mm). The overnight broth culture of *S. aureus* (MRSA) ATCC 43300 grown in MHB was centrifuged at 3500 rpm for 15 min, washed with PBS and resuspended to obtain a final density of approximatively 1–4 x 10^6 CFU/mL. The standardized bacterial suspension (300 μL) was inoculated onto the surface of the DAC samples, ensuring the surface was covered. Upon the 300 μL volume addition pursued with the bacterial inoculum onto 50 mg hydrogel, the theoretical concentration of the drugs was diluted as follows: Cur to 0.143 mg/g and Van to 0.0054 mg/g.

After irradiation treatment (30 min), the cell count was performed by serial dilutions in PBS, drop-plated on MHA, incubation at 37 °C for 24–48 h and subsequent colony count expressed as log CFU/mL. Subsequently one set of disks was incubated at 37 °C for 24 h in a humid chamber, the other set of disks was added with MHB (300 μL) and incubated at the same conditions.

After 24 h-incubation, the effect of different DAC samples (with and without MHB) was evaluated by collecting residual bacteria to the disk surface using sterile mini-scrapers; all samples were then vortexed to resuspend the harvested bacteria and each suspension was serially diluted to determine CFU per disk, as reported above. Undiluted samples were also seeded on MHA plates. The corresponding sets of disks were kept in the dark (30 min) and then incubated as described above.

Subsequently, the Cur-DAC sample was analysed also against *E. faecium* DSM 17050 (VRE-fm) and *P. aeruginosa* ATCC 9027.

2.9.4. Statistical analysis

Results were expressed as the mean value ± standard deviation from three experiments. A two-way analysis of variance (ANOVA) was used to determine significant differences between the samples after light irradiation compared with samples in the dark. Multiple comparisons were performed among groups by the Bonferroni correction test. The results with a p-value ≤ 0.05 were considered statistically significant.

3. Results and discussion

3.1. Hydrogel preparation

In clinical applications, DAC is usually prepared at 3 or 6 % (w/w over water) that is supplied, depending on the choice of the surgeon, with a selected antibiotic ranging from 20 to 50 mg/mL (that is from 18.8 mg to 45.8 mg per mg of DAC prepared at 3 % w/w) and/or an anti-inflammatory drug (Romano et al., 2016).

With the aim of exploiting a preventive irradiation of the titanium prosthesis coated with antibacterial hydrogel by photoactivating Cur before implantation and, after implantation gradually release both Cur and Van to reduce the onset of PJI, two main typologies of DAC-based hydrogels were produced: i) Cur-loaded DAC (Cur-DAC); ii) Cur- and Van- loaded DAC (Cur/Van-DAC). The hydrogels were prepared following a two-syringe-mixing technique as reported in the experimental section, to mimic the extemporaneous preparation used in clinical settings. The preparation procedure is schematized in Fig. 1.

The produced formulations are summarized in Table 1 including Cur-DAC prepared without Van, Cur/Van-DAC, Van-DAC prepared without Cur, DAC prepared without any drugs at standardized concentrations. The theoretical amount of Van used was 0.0384 mg/g, around three orders of magnitude lower than the conventional dosage used in clinics. On the other hand, purified Cur (see from Fig. S1 to Fig. S3 for analytical data) was loaded using a theoretical amount of 0.96 mg/g and 0.48 mg/g. Cur was chosen because it is GRAS natural molecule that can have promising beneficial actions on bacterial infections (Mun et al., 2013; Strimpakos and Sharma, 2008). Previously published data reports that the antibacterial properties of Cur were mainly focused on Gram-positive bacteria in both static (darkness) and light-irradiated conditions, in the latter case the action is greater but are not simply manageable in the biological media because of dramatically low solubility in water (Adamczak et al., 2020; Condat et al., 2015; Shome et al., 2022). To incorporate Cur in the DAC hydrogel, a cosolvent such as propylene glycol (PG) was used. PG was chosen because is a safe and GRAS solvent, highly miscible with water, and commonly used as food additive in many pharmaceutical formulations (Fowles et al., 2013). Moreover, PG was able to solubilize the Cur, allowing also miscibility with water without causing Cur precipitation at the maximum concentration used (0.96 mg/g). The incorporation of Van was performed in ultrapure water, given its high-water solubility.

Furthermore, Table 1 reports samples A, C, D containing lower amounts of Cur, Van or DAC that were used as model systems for interaction, colloidal and photostability studies together with DAC 1 % sample that was used as a reference in rheological investigations. We anticipate that by considering the 1 % w/w DAC formulation is not used in the clinical practice since it has not guaranteed adequate spreadability onto titanium prosthesis, the hydrogels formulated with DAC 3 % w/w and Cur ~ 1 mg/g were selected to continue the technological and biological investigations. Hence the complete hydrogel Cur/Van-DAC was formulated by using the highest Cur concentration (~ 1 mg/g) by considering its solubility in PG/H_2O, and an amount of Van (≅ 0.038 mg/g), that after 1/10 dilution in the selected medium performed for microbiological investigation, is fairly above the recognized MIC of 0.001 mg/mL (that is 0.001 mg/g water).

Cur/Van-DAC 0.5 and Van-DAC 0.5 were also prepared to compare the antibacterial effectiveness even at lower amount of vancomycin to Cur/Van-DAC and Van-DAC. As for the other samples, the Cur concentration was set at ~ 1 mg/g, while for Van at ~ 0.005 mg/g, that after a 1/10 dilution in the selected medium, is below the MIC.

The loading of Cur and Van within the DAC-based hydrogels was estimated using spectrophotometry and HPLC respectively (*see materials and methods section for details*). Due to the appreciable extinction coefficient of Cur in the visible region, the spectrophotometric quantification was easy and accurate. Cur was isolated from Cur-DAC and Cur/Van-DAC by solvent extraction with methylene chloride (DCM) and quantified by UV/Vis absorption ($\varepsilon_{419\ nm\ (DCM)} \sim 47740\ M^{-1}cm^{-1}$ (Zagami et al., 2023)). It was found that the Cur concentration into the hydrogel was 0.9325 mg/g with 0.0932 % of actual loading and an entrapment efficiency around 97 %. Due to insolubility in organic solvents and to the large absorption of DAC in the UV region the same method was not suitable for Van determination. An HPLC method was performed with Cur/Van-DAC and Van-DAC, finding a Van concentration of 0.0334 mg/g, the actual loading of around 0.003 % and 87 % of entrapment efficiency (see Table S1, Fig. S4 and Fig. S5).

3.2. Rheological investigation

An important characteristic of DAC is its rheology, which is compliant to mechanical stress and guarantees a prosthesis covering ability after extrusion (Giammona et al., 2018). To pursue this aim rheological characterization of the DAC-based hydrogels (at different

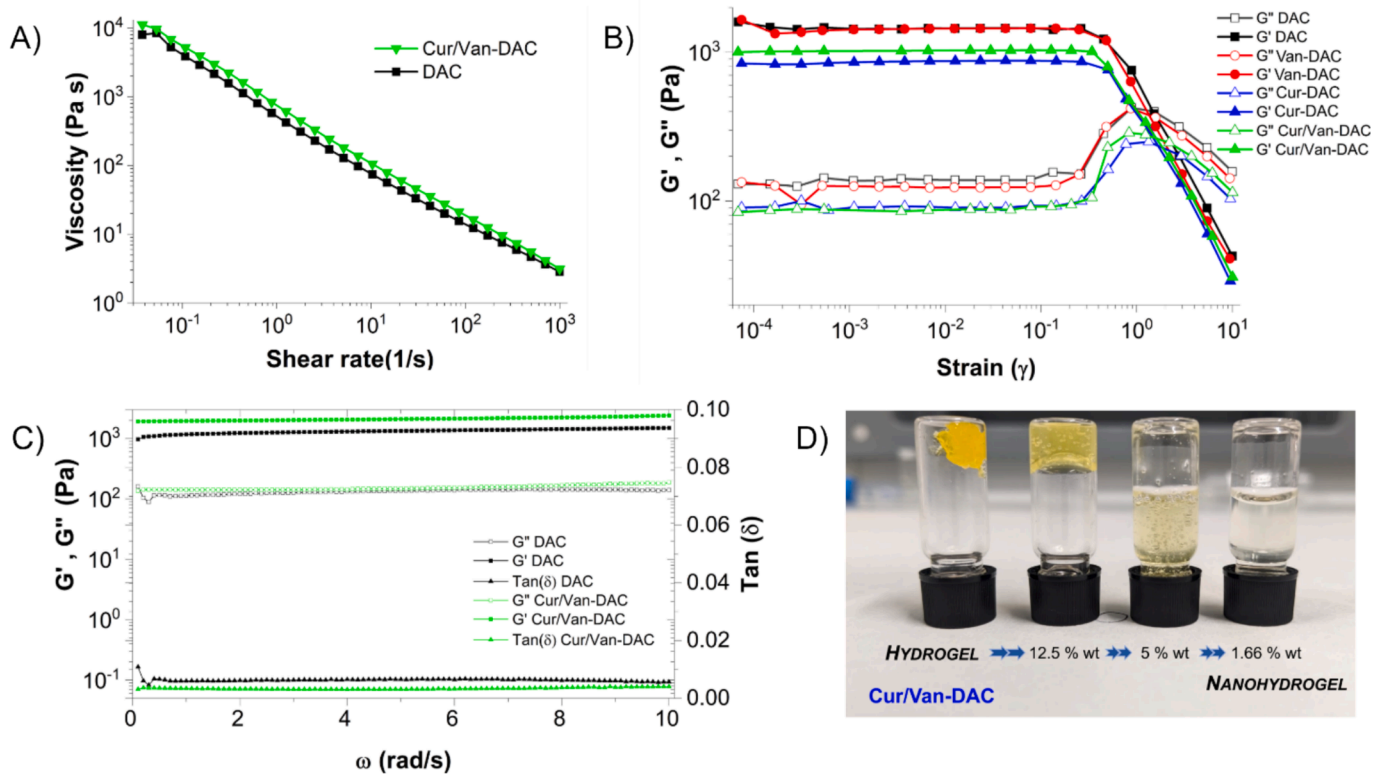

Fig. 2. A) Steady-state flow curves of DAC and Cur/Van-DAC (shear rate range 0.03–1000 s^{-1}); b) Amplitude sweep of DAC, Cur-DAC, Van-DAC and Cur/Van-DAC (strain range: 0.1–1000 % at frequency 10 rad/s); c) Frequency Sweep of DAC and Cur/Van-DAC (strain: 1 % frequency range 1–20 rad/s); d) Cur/Van-DAC inverted vials micrographs at 25 °C from hydrogel (100 % w/w) to nanohydrogel state upon dilution in ultrapure water, on the insert the w/w % concentration of the nanohydrogel in water.

DAC concentration) were carried out and together to their micrographs are reported in Fig. 2. For Cur/Van-DAC and DAC, the results of steady state shear rate experiments plotted as viscosity curves upon shear rate are depicted in Fig. 2a. Both the samples exhibited shear-thinning behavior, typical of non-Newtonian fluids. This was indicated by the downward slope of the curves, meaning that viscosity decreases as the shear rate increases. The graph shows that they share similar shear-thinning properties (as indicated by their parallel trends), with slightly higher viscosity for Cur/Van-DAC than DAC, suggesting that Cur and Van in Cur/Van-DAC may have modified the entanglement of the DAC fibers.

Fig. S6 shows the steady-state flow curves of Van-DAC (panel a), and Cur-DAC (panel b) compared to DAC and Cur/Van-DAC, respectively. The graphs demonstrate that neither Van nor Cur individually affects the viscosity of DAC-based hydrogels but their combination in Cur/Van-DAC results in slightly higher viscosity, indicating a synergistic effect that enhances the structural properties of the hydrogel. Moreover, as can be expected DAC displayed higher viscosity than DAC 1 %, while maintaining roughly the same shear thinning behavior (Fig. S7). The experimental flow curves were fitted by a power law model, using equation 4:

$$\eta = K \bullet \dot{\gamma}^{n} \quad (Eq.4)$$

The tested samples showed a good agreement with the power law model, with good correlation coefficient ($r > 0.95$, see Table S2). This model describes the relationship between viscosity (η) and shear rate ($\dot{\gamma}$), using parameters K (consistency) and n (shear thinning index). K indicates the viscosity at a shear rate of 1 s^{-1}, and n (which is less than 1) reflects non-Newtonian shear-thinning behavior for each one formulation tested. Shear-thinning is beneficial for extrudable hydrogels, as reduced viscosity during the spreading facilitates easy extrusion from the needle, while higher viscosity at rest ensures stability on the prosthetic surface.

Amplitude and frequency sweep oscillatory tests were conducted to assess the elastic (G′) and viscous (G″) moduli (Fig. 2b). An amplitude sweep in strain control at fixed frequency (10 rad/s) was performed to evaluate the linear viscoelastic region (LVER), where materials maintain their microstructure in a range of strain or stress conditions. The limit of LVER corresponds to the point at which G' becomes strain-dependent (γ_c) due to microstructure breakage. The loading of vancomycin and curcumin I in DAC resulted (Fig. 2b) in similar LVER lengths and strain values at the material breakdown (γ_c). Looking closely at Fig. 2b, it can be seen how the loading of Van (red line) does not influence the value of G′ and G″ compared to DAC alone (black line). On the other hand, the addition of Cur (blue lines) markedly affected the value of G′ and G″ compared to DAC (black line). Intermediate behavior was shown in the simultaneous loading of Cur and Van to DAC (green lines). The LVER of DAC 1 % and DAC were also compared, with DAC showing a slightly longer LVER (Fig. S8).

The magnitude of complex moduli G* of tested samples is reported in Table S3. As can be expected, the less stiff sample was DAC 1 %, while the more structured one was DAC. These findings were confirmed with a visual inspection by inverted vials test on Cur-Van/DAC hydrogel upon dilution (Fig. 2d).

Frequency sweep measurements were carried out to evaluate the behavior and inner structure of polymers, focusing on the tan(δ) phase angle (see Fig. 2c and Fig. S9). For materials where G' significantly exceeds G“, the value of tan(δ) approaches 0, indicating a dominant elastic response (or gel behavior). Conversely, for viscous materials where G' is less than G”, tan(δ) exceeds 1. The experiments showed that DAC and Cur/Van-DAC formulations exhibited gel behavior, maintaining consistent properties across frequencies range. G' was higher than G“ by one order of magnitude with the loss factor (tan δ) less than 0.1 (see Fig. 2c) indicating strong gel characteristics, thus allowing them to retain their shape despite the applied deformation stress.

Altogether, oscillation tests showed that all the formulations presented strong gel behavior. This was due to their elastic response G′ was constant in the range of tested frequencies, a ratio of one magnitude order between elastic and viscous moduli was found and a loss factor (tan δ) proximally to 0 was recorded. Interestingly, the presence of only Cur in the hydrogel affected the G' and G“ values of the DAC control. It meant that Cur could decrease the strength of the hydrogel, facilitating its extrusion. This result also provides indirect evidence of the significant interaction of Cur within the hydrogel. On the other hand, loading only Van at the concentrations set for this work did not seem to change the hydrogel properties, differently from other reports where Van was loaded at higher concentrations into HA-based hydrogels (Huang et al., 2018).

3.3. Morphological and colloidal characterizations of the nanohydrogel

The Cur/Van-DAC hydrogel was diluted to 0.83 % w/w in ultrapure water for spectroscopic, colloidal, and morphological characterizations. Upon dilution, it assumes a nanohydrogel morphology. Fairly, it represents the erosion product found during the release/erosion studies and the one that is generated once it is implanted together with the prosthesis *in vivo*. The morphology of the nanohydrogel was investigated by Atomic Force Microscopy (AFM). The result highlights the presence of a network of globular-like structures characterized by the existence of pores with diameters ranging from 5 to 20 nm, evenly distributed over the analysed area (Fig. 3a, 3c). The line profile (Fig. 3d) reveals that the film thickness is approximately 2 nm. Interestingly, the hydrogel network upon excitation at 473 nm, exhibits the typical photoluminescence of Cur entrapped in DAC (Fig. 3b) similarly to Cur-DAC nanohydrogel dispersion (*vide infra)*.

The colloidal stability of Cur-DAC nanohydrogel over time intervals from 24 h to 144 h at 4 °C and 37 °C was investigated and compared to Cur/Van-DAC and Van-DAC respectively. All the systems were investigated upon dilution of the initially formulated hydrogels (see Table 1) to 0.83 % w/w in water. The double-Y graphs show the average hydrodynamic diameter (D_H) estimated by Dynamic Light Scattering (DLS) and the ζ-potential values acquired at different temperature and plotted against time (Fig. 3e and Fig. 3f). In Fig. S10 graphs for all the produced hydrogels are reported, including the complete colloidal stability data in Table S4.

On freshly prepared and room temperature (R.T. ~ 25 °C) equilibrated samples D_H was ~ 230 nm with a minority population (10 %) of ~ 20 nm and the average ζ-potential was ~ -40 mV suggesting high stability of the colloidal dispersion (Fig. 3g and Fig. 3h). Despite the stability of the nanohydrogels (ζ-potential stated around −40 mV for all the investigated nanohydrogels), the D_H was affected by time and temperature. Temperature seems to affect Cur-DAC more while Cur/Van-DAC shows minor temperature dependence. In fact, from an initial value of ~ 150 nm the D_H of Cur-DAC stored at 4 °C reached 600–700 nm only at 72 h, while that stored at 37 °C reached this size already at 24 h. On the other side, the Cur/Van-DAC samples stored at 4 and 37 °C followed a similar aggregation trend (D_H from ~ 250 to 1100 nm) until 72 h, changing their behavior at 144 h where the 37 °C sample was much more aggregated (~3.3 μm). The freshly prepared and diluted Van-DAC nanohydrogel showed D_H around ~ 380 nm, which is fairly maintained if it is stored at 4 °C for 24 h. The increase of temperature strongly affected the aggregation behavior of the latter nanohydrogel. In order to compare the colloidal behavior of the nanohydrogels vs their concentration, by maintaining constant DAC amount at 0.025 % w/w, the systems A and C were freshly formulated and investigated (A and C at 2.5 % w/w vs Cur-DAC, Cur-Van/DAC and Van-DAC at 0.83 % w/w nanohydrogel/water). Also sample D was prepared and diluted at 0.83 % w/w nanohydrogel/water. D_H and ζ-potential of these nanohydrogel are also reported in Table S4. As expected, at all the investigated temperatures, the higher hydrogel concentration (as in A and C), the higher D_H with a significative tendency to form microstructures was found. Interestingly, ζ-potential is maintained at high negative values for all the

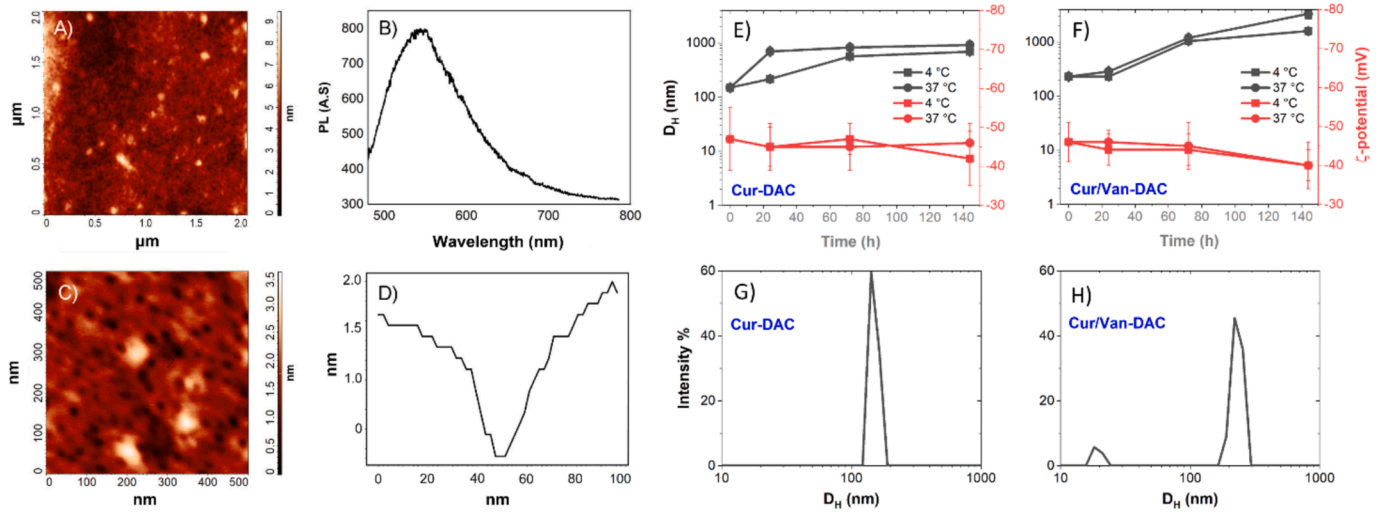

Fig. 3. A-d) AFM characterization of Cur/Van-DAC nanohydrogel: a) Morphology on 2x2-micron square area; b) The emission spectrum from the centre of the analysed area by exciting with a 473 nm DPSS laser; c) Zoomed-in view of the surface to highlight its nanoscaled structure, the continuous black line in the image represents the path along which the profile, shown in Fig. 2d, was obtained; d) Profilometry. e-f) Colloidal stability investigation by D_H and ζ-potential over the time (0–140 h) of Cur-DAC (e) and Cur/Van-DAC (f) nanohydrogels (diluted to 0.83 % w/w) at different temperature (4 and 37 °C). D_H distribution of Cur-DAC (g) and Cur/Van-DAC (h) nanohydrogels at 0.83 % w/w freshly prepared and equilibrated at room temperature.

investigated nanohydrogel samples pointing out stability of the formulation till 144 h. In conclusion, Cur-DAC and Cur/Van-DAC nanohydrogels prepared upon dilution of freshly formulated hydrogels can be stored at 4 °C till to 144 h by showing good stability in this time interval.

3.4. *Spectroscopical characterization and photostability*

By considering that the overall goal was to carry out a preventive irradiation of the prosthesis coated with Cur/Van-DAC hydrogels, the photostability of Cur within our hydrogel formulations was investigated. A fully spectroscopic study was conducted on hydrogel diluted to nanohydrogels which mimic the erosion products in biologically relevant media. UV/Vis absorption spectroscopy displayed the dynamics of Cur within different solvents/media both in static and in light irradiation conditions, the latter to evaluate the photodegradation kinetics. Fig. 4 includes normalized UV/Vis (Fig. 4a) absorption and (Fig. 4b) emission spectra of Cur in DCM, PG, PG/H_2O and in the Cur/Van-DAC nanohydrogel system.

As reported by literature (Patra and Barakat, 2011), in non-polar solvents as DCM the absorption spectrum of Cur exhibits the vibronic structure with the main electronic transition around 418 nm. Experiencing polar and protic environments causes the prevalence of the keto tautomeric form of Cur towards the enolic form due to preferential intermolecular hydrogen bonding and the loss of the vibronic patterns (Laneri et al., 2023) in the absorption spectrum, as happened for the spectra recorded in PG and PG/H_2O. The absorption maximum is shifted to higher wavelengths (~ 432 nm) in PG, whereas in PG/H_2O there is also a shoulder around 365 nm which might be associated to the water-induced shift of the tautomeric equilibrium to the di-keto form (Moussa et al., 2017). The absorption spectrum of the nanohydrogel is represented by the typical light scattering of nanoaggregates, accompanied by significant broadening of the band, blue shift of the maximum to 410 nm and a new peak around 510 nm. Looking at the emission spectra, the Stokes shift increases as the polarity of the environment (Fig. S11) attempting the largest in the nanohydrogel. In the Cur/Van-DAC nanohydrogel spectrum the main emission maximum is around 555 nm, but another peak around 480 nm is detected. Again, this secondary band might be associated to residual emission of the keto tautomeric forms of Cur in water. Notwithstanding the blue shift of the maximum and the broadening of the absorption band may be reasonable indications of the interaction of Cur within the nanohydrogel network, another evidence supporting the interaction is the detection of an absorption peak at 510 nm – exclusively present in the spectrum of the nanohydrogel – that is attributed according to literature (Adhikary et al., 2010) to a deprotonated species of Cur. In water Cur is involved in acid-base equilibria, but most of the population in the pH range 1–7 is in the neutral form (Borsari et al., 2002; Tsuda, 2018). The first dissociation happens when pH > 7.5, the pK_a value 7.75–7.8 is related to the dissociation of the enolic proton which drives rapidly the molecule (the half-life is calculated to be less than 10 min) to degradation reactions mainly to ferulic acid and feruloylmethane (Priyadarsini, 2009). As clarified by the absorption spectrum, the deprotonated specie is only minority and stable over the

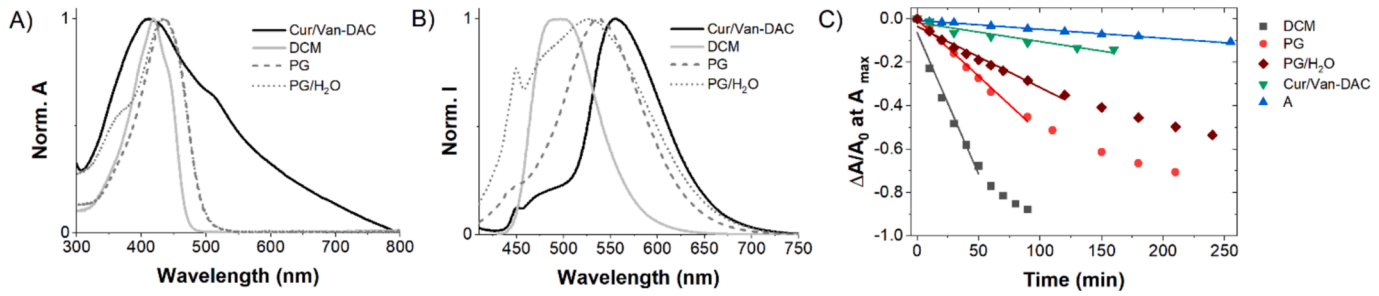

Fig. 4. A) Normalized UV/Vis absorption spectra and b) normalized emission spectra (λ_{exc} = 390 nm) of Cur in different solvents (DCM, PG, PG/H_2O) and within Cur/Van-DAC hydrogel; c) Absorbance differences as a function of the irradiation time (0 to 90–255 min) of Cur in different solvents (DCM, PG, PG/H_2O), within Cur/Van-DAC 0.83 % w/w and A 2.5 % w/w nanohydrogels.

time as confirmed by the absorption spectra of the nanohydrogels recorded during the colloidal stability tests at 4 °C and 37 °C for 6 days. In Fig. S12 and Fig. S13 the absorption spectra normalized for the scattering at 800 nm elucidate the stability of the absorption ratio between the peak at 418 nm (Cur) and the one at 510 nm (deprotonated Cur) over the time. Consistent with our results, it seems that the DAC-based hydrogel had protective effects on Cur from pH-induced degradation reactions blocking the progression of the metastable deprotonated form. In addition, the molar extinction coefficient of Cur incorporated into the DAC-based nanohydrogels (Fig. S14), apart from usual experimental fluctuations, was not substantially affected by the concentration of DAC (3 % or 1 % w/w), by the dilution and by the presence of Van. This should be considered as important evidence of the stability of the formulation in the aqueous medium preventing from Cur precipitation.

To assess whether the DAC-based hydrogels could also have a protective effect from Cur photodegradation reactions, photostability experiments were performed. Results from Cur/Van-DAC and sample A nanohydrogels (see Table 1) were compared to solutions of Cur. The nanohydrogel A demonstrated increased photostability compared to the solutions of Cur in DCM, PG and PG/H_2O of around 30, 12 and 7 times respectively (Fig. 4c). In instance, this could be explained by some trivial effects related to the dynamics of the absorption of light photons. In our case, to a small extent due to the slight absorbance difference (~ 10 %) between the samples which misalign the absorbed fraction. To a greater extent, by the light scattering operated by the nanoscopic hydrogel responsible of diffusion, thus limiting the absorbable fraction. A second explanation is more related to the protective effect of a rigid system, as the DAC network, on the freedom degrees of Cur. Reducing the molecular mobility both in the ground and in the excited states reduces the collision probability to the environment, thus limiting degradation. In fact, as reported for the binding of Cur inside the hydrophobic pockets of albumin, the molecule can form intermolecular H-bonds with the host system and the water molecules confined in it (Laneri et al., 2023; Pulla Reddy et al., 1999). Notwithstanding the superior stability, Cur/Van-DAC showed very similar trend as the A nanohydrogel. This was introduced in the experimental evaluations since the 0.83 % w/w Cur/Van-DAC in water showed more than 80 % on absorbance difference at 450 nm compared to the Cur solutions. Indeed, maintaining unaltered the concentration of DAC (0.025 % w/w) the concentration of A in water is 0.25 % w/w and the Cur concentration ~ 62 μM having an absorbance at 450 nm more similar to the Cur solutions. In Fig. S15 the complete absorption changes over the irradiation time are reported. As long as the illumination occurred the main absorption band lost in intensity, while prolonging the illumination an absorption peak around 360–370 nm appeared, that could be attributed to some photodegradation product. The results of the photodegradation rate of Cur in the hydrogel assured that the system is exploitable for antimicrobial photodynamic therapy. Cur has *per se* antibacterial action in darkness condition but was extensively studied for its photoinduced effects. Recently, Sortino's research group (Laneri et al., 2023) reviewed and investigated the phototoxic effects of Cur in biocompatible hosts. They demonstrated thanks to photophysical investigations that in aqueous environment Cur is largely present in the di-keto tautomeric form that exhibit the typical photoreactivity of carbonyl compounds. The photogenerated triplet excited state leads to the formation of a ketyl radical for a proton abstraction process from the environment. The photo-generated toxic species of Cur have been identified in the radical recombination product that could be intra-host covalent products or peroxyl radical species.

3.5. Kinetic erosion profiles

Kinetic erosion profiles of Cur/Van-DAC, Cur-DAC and Van-DAC hydrogels were evaluated in physiological conditions (pH 7.4, 37 °C) using the cumulative drug release method (Fig. 5 and Fig. 6). When in contact with the aqueous phase, DAC-based hydrogels assume

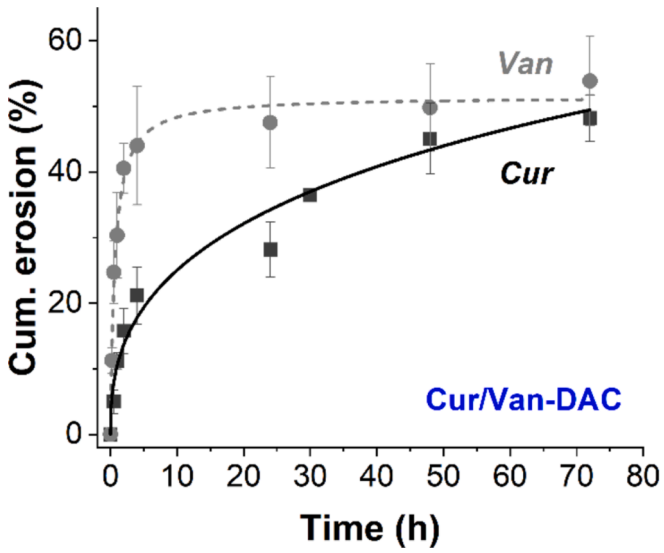

Fig. 5. Kinetic erosion profile of Cur/Van-DAC. Data were obtained by spectrophotometric determination of Cur within the eroded nanohydrogel and by HPLC determination of released Van from and within the nanohydrogel. The Cur curve was fitted using the Peppas-Sahlin's model whereas the Van curve was fitted using the Hagen's model.

nanohydrogel morphology (see Fig. 3a-d) that mimic the erosion product once they are implanted together with the prosthesis. In the nanohydrogel, hydrophobic drugs such as Cur continue to be dispersed within the polymer network, while hydrophilic drugs such as Van might be both released in physiological medium and dispersed into the nanohydrogel. Indeed, during the erosion studies of the hydrogels we found that in the receiving PBS phase at 37 °C it is possible to observe the typical UV/Vis absorption of Cur entangled within the nanohydrogel without any precipitation of Cur. Therefore, the amount of Cur within the eroded nanohydrogel was spectrophotometrically estimated. Instead, the amount of Van released from the hydrogel or within the eroded nanohydrogel was estimated by HPLC method from reconstitution in ultrapure water of the freeze-dried receiving phase.

Fig. 5 depicts the erosion profile of Cur/Van-DAC monitoring the kinetics of Cur and Van. The experimental data from the two profiles were fitted using different mathematical models. The profile of Cur was fitted with the Peppas-Sahlin's model, while that of Van with the Hagen's model (Lu and Ten Hagen, 2020). However, both the systems showed a mixed kinetic pursuing a burst effect in the first 4 h, followed by slower and steadier erosion in the time interval 24–72 h. Like the Peppas-Sahlin's the Hagen's model was also built to interpret the behaviour of systems with multiple drug release mechanisms. They consider a macroscopic biphasic release – which is explained by complex mechanisms underlying polymer dynamics in solution – introducing some modifications on the exponential equation. The Hagen's model in particular was created to fit the temperature-induced ultrafast burst release from small thermoresponsive liposomes (Lu and Ten Hagen, 2020). In the case of this work, at the end of the determination (72 h) the amount of drugs released or within the eroded Cur/Van-DAC nanohydrogel was around 50 % of the incorporated fraction in the initial hydrogel. Basically, the majority of Van (~ 44 %) was detected during the burst effect of the first 4 h. Instead, only ~ 20 % of Cur was found during phase steadily reaching ~ 48 % in the following 68 h. This trend can be rationalized considering the different solubility of the drugs. In any case, the burst effect might be probably controlled by the temperature, after preparation the hydrogel in fact passed from room temperature to 37 °C and this reasonably affected the polymer dynamics of the drug reservoir system. In fact, for the greater extent, the nanohydrogel formation occurred in this phase. While, taking into account the water

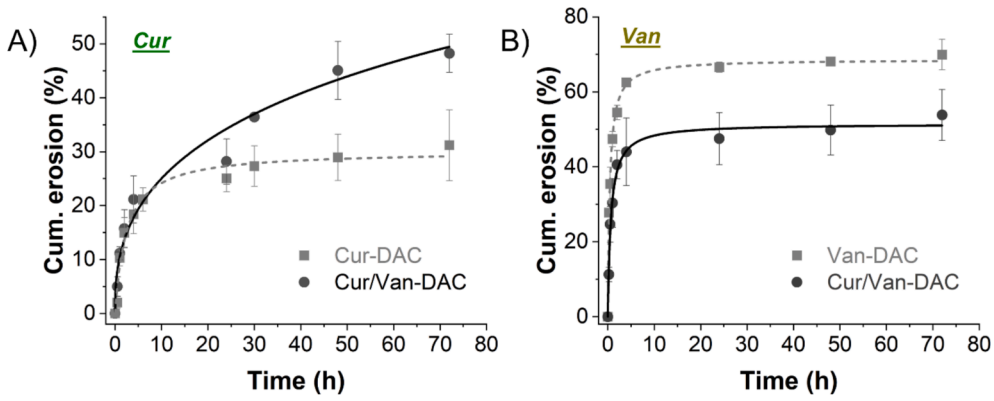

Fig. 6. Comparison of kinetic erosion profiles of Cur/Van-DAC with Cur-DAC, looking at the quantitative determination of Cur (a) and between Cur/Van-DAC and Van-DAC, looking at the quantitative determination of Van (b). Cur was determined by UV/Vis and Van by HPLC (see materials and methods section). The kinetic curves of Van (b) and the kinetic curve of Cur from Cur-DAC (a) were fitted using the Hagen's model, while the kinetic curve of Cur from Cur/Van-DAC (a) with the Peppas-Sahlin's model.

solubility of Van, it appears that in the meantime of the nanohydrogel formation Van was released into the aqueous receiving phase due to multiple mechanisms (diffusion, swelling, erosion) preserving the residual percentage inside the hydrogel matrix. The case of Cur is different because of the water insolubility. The experimental results may be only explained by the hydrogel erosion. As a result, during the burst effect around 20 % of Cur was found and Cur continued over the time until around 48 % to be dispersed in water thanks to the embedding into the nanohydrogel.

The erosion/release experiments were also performed for Cur-DAC and Van-DAC (Fig. 6 and Figs. S16-S19). Table S5 resumes the parameters values obtained by the fitting of the experimental data from the three hydrogels with five different mathematical models: first order (simple exponential), Higuchi's, Korsmeyer-Peppas', Peppas-Sahlin's and Hagen's. According to the table, the best fitting for Cur-DAC and Van-DAC was Hagen's by comparing the correlation coefficient (R^2).

Fig. 6a shows the comparison of the quantitative determination of Cur from Cur/Van-DAC and Cur-DAC erosion, while Fig. 6b the comparison of the Van determination from Cur/Van-DAC and Van-DAC erosion. Kinetic profiles of Van in Van-DAC and in Cur/Van-DAC were both fitted with the Hagen's model, but they showed a different amount of drug in the receiving phase at the end of determination of about 70 % and 54 % respectively. The magnitude of this difference was focused on the burst phase which could be explained by the increase in the steric hindrance or by some supramolecular interactions provided by the insertion of Cur in the polymer matrix that limited the extent of Van diffusion. This provides further evidence of the leading role of diffusion on the delivery mechanism of Van from DAC-based hydrogels. On the other hand, the kinetic profiles of Cur in Cur-DAC and in Cur/Van-DAC are suggesting a more complex behaviour. In fact, they are differing for the second and slower phase of the erosion profile. The curve coming from Cur-DAC was fitted keeping the model already used for Van, while the one coming from Cur/Van-DAC with the Peppas-Sahlin's. Due to a mechanism that is not yet fully understood, it seems that the presence of Van can influence the amount of eroded Cur within nanohydrogel with respect to Cur-DAC.

3.6. *Antibacterial and photo-antibacterial efficacy of DAC-based nanohydrogels*

Since the photostability studies of Cur in the nanohydrogel assessed that the system is exploitable for antimicrobial photodynamic therapy, antibacterial and photoantibacterial tests were performed. First of all, the antibacterial activity of curcumin-based systems was evaluated. Results are reported in Table S6. Notably, the solution of Cur in PG demonstrated higher efficacy against all bacteria (MIC/MBC values ranging from 0.062 mg/mL to 0.5 mg/mL) compared to the DMSO solution (MIC/MBC values ranging from 0.125 mg/mL to > 2 mg/mL). Furthermore, in accordance with literature reports Cur in DMSO and PG solutions was more effective against Gram-positive than Gram-negative bacteria (Table S6) (Adamczak et al., 2020). This is thought to be probably due to differences in cell wall structure and composition. Gram-negative bacteria have an outer phospholipid membrane with lipopolysaccharide components that provides an additional selective permeability barrier. Cur-DAC systems did not show any antibacterial activity to all the tested concentrations (correspondently to concentration lower than MIC of Cur in PG, see Table S6). Indeed, it was not possible to test Cur-DAC and Cur/Van-DAC at concentration of Cur that were equal or higher than the MIC value due to the dilution required to obtain a well-dispersible system to perform antibacterial tests.

Hence with the aim to improve the antibacterial activity of Cur-DAC based systems, experiments to explore antimicrobial photodynamic activity were conducted. The methicillin-resistant *S. aureus* (MRSA) ATCC 43300 and *P. aeruginosa* ATCC 9027 strains were selected as Gram-positive and Gram-negative bacterial models to evaluate the efficacy of Cur solution in PG and Cur-DAC after irradiation treatment. In this set-up, results confirm the photosensitizing properties of Cur (Fig. 7). Significant reduction of initial MRSA load (1.8 x 10^6 CFU/mL) was caused by Cur in PG and Cur-DAC upon light, reaching adecrease in CFU/mL equal to 99.9 % and 99.4 % corresponding to 3 and 2.2 log reduction, respectively (Fig. 7a). In contrast, poor antibacterial effects were detected in the dark. Although to a lesser extent, Cur in PG and Cur-DAC after irradiation showed bactericidal activity against *P. aeruginosa* ATCC 9027 compared to lack of activity when they were kept in the dark (Fig. 7b). Specifically, the initial bacterial load (3.5 x 10^6 CFU/mL) was reduced by about 87.7 % (0.91 log reduction) and 77 % (0.64 log reduction) in CFU/mL. This behaviour agrees with the lower susceptibility of Gram-negative to Cur-based systems. No significant ($p > 0.05$) activity was demonstrated by a PG alone and DAC samples.

3.6.1. *Antibacterial and photo-antibacterial efficacy of DAC-based hydrogels on spread titanium disks*

The effect of different DAC-based hydrogels spread on titanium disks against MRSA and *E. faecium* DSM 17050 (VRE-fm) is shown in Fig. 8 and Fig. 9. Titanium disks with material specifies mimicking prosthesis were utilized. As above mentioned, since the DAC-based hydrogels with DAC 1 % w/w has not guaranteed adequate spreadability on titanium disks, the hydrogels formulated with DAC 3 % w/w (Cur/Van-DAC and Van-DAC containing Cur ≅ 0.93 mg/g and or Van ≅ 0.033 mg/g) were selected for the following antibacterial investigations. Furthermore, Cur/Van-DAC 0.5 and Van-DAC 0.5 were chosen to compare the antibacterial effectiveness of lower amount of vancomycin to Cur/Van-DAC

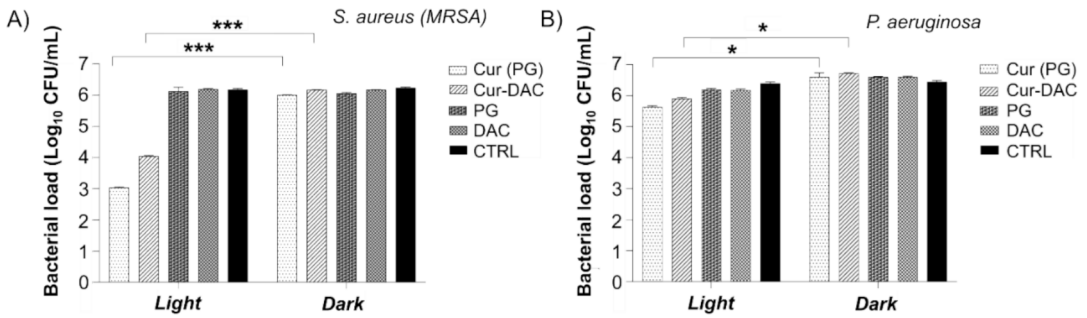

Fig. 7. Effects of Cur in PG and Cur-DAC after light irradiation (30 min) and in the dark on load of *S. aureus* (MRSA) ATCC 43300 (a) and *P. aeruginosa* ATCC 9027 (b). All data are presented as mean ± SD (* $p \leq 0.05$; *** $p \leq 0.001$).

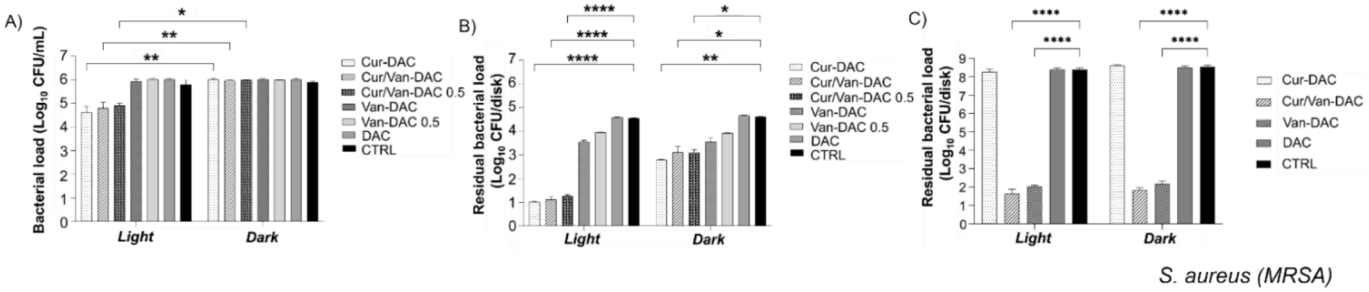

Fig. 8. Effects of DAC-based hydrogels spread on titanium disks on *S. aureus* (MRSA) ATCC 43300 under light irradiation (30 min) and in the dark (a), subsequent 24 h incubation at 37 °C without MHB (b) and with MHB (c). All data are presented as mean ± SD (* $p \leq 0.05$; ** $p \leq 0.01$; **** $p \leq 0.0001$).

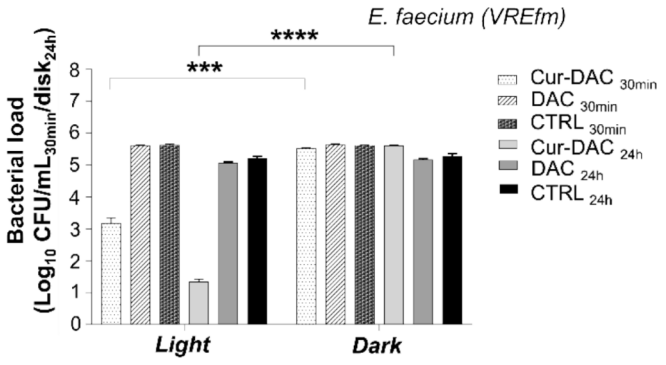

Fig. 9. Effects of DAC-based hydrogels spread on titanium disks on *E. faecium* DSM 17050 (VREfm) under light irradiation and in the dark (30 min) and subsequent 24 h-incubation at 37 °C. All data are presented as mean ± SD (*** $p \leq 0.001$; **** $p \leq 0.0001$).

and Van-DAC.

A significant reduction of initial bacterial load (1.2 x 10^6 CFU/mL) was detected with Cur-DAC, Cur/Van-DAC and Cur/Van-DAC 0.5 irradiated for 30 min when compared to the corresponding samples kept in the dark. The reduction attained was 96.48 % (1.45 log decrease), 94.66 % (1.28 log decrease) and 93.25 % (1.18 Log decrease), respectively (Fig. 8a). No significant ($p > 0.05$) reduction was found for Van-DAC and Van-DAC 0.5, either under irradiation or in the dark (Fig. 8a). Regarding the results after 24 h of incubation, again Cur-DAC and Cur/Van-DAC were the best samples in reducing MRSA viability by 99.999 % (5 log reduction in CFU/mL) (Fig. 8b). However, the same samples kept in the dark caused a reduction in bacterial load of 99.9 % – 99.89 % (~ 2–3 log reduction in CFU/mL). Although to a lesser extent, even the Van-DAC samples (both irradiated and kept in the dark) displayed inhibitory efficacy (Fig. 8b). Regarding the samples of Cur/Van-DAC and Van-DAC spread on titanium disks incubated for 24 h in the presence of nutrients (MHB), the results showed the effectiveness of Cur/Van-DAC hydrogels even when kept in the dark. This could be ascribed to the Van action on cell-wall biosynthesis of actively dividing (i.e. in the presence of nutrients) Gram-positive bacteria. It is known that vancomycin binds to the acyl-D-ala-D-ala portion of the cell wall, a necessary precursor for peptidoglycan cross-linking (Rubinstein and Keynan, 2014). This hypothesis is further confirmed by the ineffectiveness of the Cur-DAC in the presence of nutrients (Fig. 8c). Probably, Cur-DAC is active only during photoactivation, whereas the remaining Cur concentration is not able to counteract the active growth of bacteria during 24 h incubation.

Based on the results obtained in the absence of nutrients, Cur-DAC hydrogel was tested against *E. faecium* DSM 17050 and *P. aeruginosa* ATCC 9027. In this case Cur/Van-DAC was not tested because *E. faecium* and *P. aeruginosa* showed MIC values of Van > 0.512 mg/mL (see Table S6). Noteworthy, in this experiment against *E. faecium* Cur-DAC reported the strongest antibacterial activity of the experimental set irradiated (Fig. 9) at 30 min and 24 h (99.7 % and 99.99 % bacterial reduction, respectively). However, the same sample was poorly active toward *P. aeruginosa* (Fig. S20).

Altogether, Cur/Van-DAC appears to be the most effective antibacterial hydrogel, as it allows a good reduction in the *S. aureus* load after 30 min of exposure to light (Fig. 8a) and a subsequent decrease of cells number at 24 h even in the presence of nutrients (Fig. 8c). Interestingly, Cur-DAC was very effective on vancomycin resistant *Enterococcus faecium* upon light treatment and following 24 h of incubation, indicating that this Cur-based hydrogel is very promising to be co-implanted with prosthesis to fight antibiotic resistant strains.

4. Conclusions

Curcumin I-loaded hydrogels based on DAC medical device were prepared by safe and reproducible protocol by using only GRAS materials. Curcumin I and vancomycin co-loaded hydrogels were also formulated. A remarkable increase of Cur solubility in DAC-based hydrogels was experienced. Oscillation tests showed that all the DAC hydrogels present a strong gel behavior with shear-thinning characteristics. This is beneficial for injectability, as reduced viscosity during

injection facilitates easy extrusion from needle, while higher viscosity at rest ensures stability on the prosthetic surface. Nanohydrogels produced from Cur-loaded and Cur/Van-loaded formulations, which represent the erosion product found during the erosion/release studies and mimicking that one generated when implanted together with the prosthesis, were prepared upon dilution of freshly formulated hydrogels. They resulted stable in aqueous colloidal dispersion at 37 °C in a time interval useful to exploit antimicrobial effect until 24–72 h. In these conditions, Cur is protected from pH-catalysed reactions, precipitation and photodegradation while maintaining photodynamic efficacy. In fact, they demonstrated increased photostability compared to the free Cur. Kinetic erosion profile of Cur-Van/DAC and Cur-DAC hydrogel showed a mixed kinetic pursuing a burst effect in the first 4 h, followed by slower and steadier erosion in the time interval 24–72 h. Antibacterial and photoantibacterial test pointed out that Cur/Van-DAC appears to be the best antibacterial hydrogel as it allows a good reduction in the *S. aureus* load after 30 min of exposure to light and a subsequent reduction of cells number at 24 h even in the presence of nutrients. Interestingly Cur-DAC is very effective on vancomycin resistant *Enterococcus faecium* upon light treatment and following 24 h of incubation, experiencing that this Cur-based hydrogel is promising to be co-implanted with prosthesis to fight antibiotic resistant strains. In perspective, this study opens the route to the development of other hydrogels entrapping photosensitisers as porphyrinoids as prosthesis coatings or in wound healing applications.

CRediT authorship contribution statement

Nina Burduja: Methodology, Investigation, Data curation. **Nicola F. Virzì:** Methodology, Investigation, Data curation. **Giuseppe Nocito:** Writing – review & editing, Writing – original draft, Visualization, Methodology, Investigation, Data curation. **Giovanna Ginestra:** Methodology, Investigation, Data curation. **Maria G. Saita:** Writing – review & editing, Methodology, Investigation, Data curation. **Fabiola Spitaleri:** Methodology, Investigation, Data curation. **Salvatore Patanè:** Methodology, Investigation, Data curation. **Antonia Nostro:** Writing – review & editing, Methodology, Investigation, Data curation, Conceptualization. **Valeria Pittalà:** Writing – review & editing, Writing – original draft, Project administration, Funding acquisition, Conceptualization. **Antonino Mazzaglia:** Writing – review & editing, Writing – original draft, Supervision, Project administration, Funding acquisition, Conceptualization.

Funding

This research was principally funded by italian MUR PON Project BONE^{++} “Development of Micro and Nanotechnologies for Predictivity, Diagnosis, Therapy and Regenerative Treatments of Pathological Bone and Osteo-Articular Alterations”, Project Number: ARS01_00693 and partially by the European Union (NextGeneration EU) through the italian MUR PNRR project SAMOTHRACE (ECS:00000022).

Declaration of competing interest

The authors declare that they have no known competing financial interests or personal relationships that could have appeared to influence the work reported in this paper.

Acknowledgements

The authors are fully grateful to Novagenit S.r.l. (Mezzolombardo, Italy)) to have provided DAC®.

Appendix A. Supplementary data

Supplementary data to this article can be found online at https://doi.org/10.1016/j.ijpharm.2025.125283.

Data availability

No data was used for the research described in the article.

References

(CLSI), C.L.S.I., 2020. Performance Standards for Antimicrobial Susceptibility Testing. 30th ed. CLSI supplement M100. Clinical and Laboratory Standards Institute, Wayne, PA-USA.

Abbas, A., Barkhouse, A., Hackenberger, D., Wright, G.D., 2024. Antibiotic resistance: A key microbial survival mechanism that threatens public health. Cell Host & Microbe 32, 837–851.

Adamczak, A., Ozarowski, M., Karpinski, T.M., 2020. Curcumin, a Natural Antimicrobial Agent with Strain-Specific Activity. Pharmaceuticals (Basel) 13.

Adhikary, R., Carlson, P.J., Kee, T.W., Petrich, J.W., 2010. Excited-state intramolecular hydrogen atom transfer of curcumin in surfactant micelles. J Phys Chem B 114, 2997–3004.

Ahmed, M.O., Baptiste, K.E., 2018. Vancomycin-Resistant Enterococci: A Review of Antimicrobial Resistance Mechanisms and Perspectives of Human and Animal Health. Microb Drug Resist 24, 590–606.

Bingyun Li, T.F.M., Webster, T., Xing, M., 2020. Racing for the surface. Antimicrobial and interface tissue engineering, Springer Nature Switzerland AG, Cham, Switzerland.

Borsari, M., Ferrari, E., Grandi, R., Saladini, M., 2002. Curcuminoids as potential new iron-chelating agents: spectroscopic, polarographic and potentiometric study on their Fe(III) complexing ability. Inorganica Chimica Acta 328, 61–68.

Condat, M., Mazeran, P.E., Malval, J.P., Lalevée, J., Morlet-Savary, F., Renard, E., Langlois, V., Abbad Andalloussi, S., Versace, D.L., 2015. Photoinduced curcumin derivative-coatings with antibacterial properties. RSC Advances 5, 85214–85224.

Dias, L.D., Blanco, K.C., Mfouo-Tynga, I.S., Inada, N.M., Bagnato, V.S., 2020. Curcumin as a photosensitizer: From molecular structure to recent advances in antimicrobial photodynamic therapy. Journal of Photochemistry and Photobiology C: Photochemistry Reviews 45, 100384.

Drago, L., Boot, W., Dimas, K., Malizos, K., Hansch, G.M., Stuyck, J., Gawlitta, D., Romano, C.L., 2014. Does implant coating with antibacterial-loaded hydrogel reduce bacterial colonization and biofilm formation in vitro? Clin Orthop Relat Res 472, 3311–3323.

Fowles, J.R., Banton, M.I., Pottenger, L.H., 2013. A toxicological review of the propylene glycols. Crit Rev Toxicol 43, 363–390.

Franceschini, M., Sandiford, N.A., Cerbone, V., Araujo, L.C.T., Kendoff, D., 2020. Defensive antibacterial coating in revision total hip arthroplasty: new concept and early experience. Hip Int 30, 7–11.

Fraval, A., Zhou, Y., Parvizi, J., 2024. Antibiotic-loaded cement in total joint arthroplasty: a comprehensive review. Archives of Orthopaedic and Trauma Surgery 144, 5165–5175.

Giammona, G., Pitarresi, G., Palumbo, F., Romanò, C.L., Meani, E., Cremascoli, E., 2010. Hyaluronic acid based hydrogel and use thereof in surgery. R.L., NOVAGENIT S.R.L., IT, ES, EP, US, WO, MERO S.

Giammona, G., Pitarresi, G., Palumbo, S.F., Maraldi, S., Scarponi, S., Romanò, L.C., 2018. Hyaluronic-Based Antibacterial Hydrogel Coating for Implantable Biomaterials in Orthopedics and Trauma: From Basic Research to Clinical Applications, in: Sajjad, H., Adnan, H. (Eds.), Hydrogels. IntechOpen, Rijeka, p. Ch. 9.

Huang, F., Cai, X., Hou, X., Zhang, Y., Liu, J., Yang, L., Liu, Y., Liu, J., 2022a. A dynamic covalent polymeric antimicrobial for conquering drug-resistant bacterial infection. Exploration 2, 20210145.

Huang, J., Ren, J., Chen, G., Li, Z., Liu, Y., Wang, G., Wu, X., 2018. Tunable sequential drug delivery system based on chitosan/hyaluronic acid hydrogels and PLGA microspheres for management of non-healing infected wounds. Mater Sci Eng C Mater Biol Appl 89, 213–222.

Huang, K., Liu, W., Wei, W., Zhao, Y., Zhuang, P., Wang, X., Wang, Y., Hu, Y., Dai, H., 2022b. Photothermal Hydrogel Encapsulating Intelligently Bacteria-Capturing Bio-MOF for Infectious Wound Healing. ACS Nano 16, 19491–19508.

Kumar, M., Kumar, R., Kumar, S., 2021. Coatings on orthopedic implants to overcome present problems and challenges: A focused review. Materials Today: Proceedings 45, 5269–5276.

Laneri, F., Conte, C., Parisi, C., Catanzano, O., Fraix, A., Quaglia, F., Sortino, S., 2023. On the photobehaviour of curcumin in biocompatible hosts: The role of H-abstraction in the photodegradation and photosensitization. J Photochem Photobiol B 245, 112756.

Lei, Z., Liang, H., Sun, W., Chen, Y., Huang, Z., Yu, B., 2024. A biodegradable PVA coating constructed on the surface of the implant for preventing bacterial colonization and biofilm formation. Journal of Orthopaedic Surgery and Research 19, 175.

Li, H., Sureda, A., Devkota, H.P., Pittala, V., Barreca, D., Silva, A.S., Tewari, D., Xu, S.W., Nabavi, S.M., 2020. Curcumin, the golden spice in treating cardiovascular diseases. Biotechnol Adv 38.

Li, J., Mooney, D.J., 2016. Designing hydrogels for controlled drug delivery. Nature Reviews Materials 1, 16071.

Liu, J., Yu, M., Zeng, G., Cao, J., Wang, Y., Ding, T., Yang, X., Sun, K., Parvizi, J., Tian, S., 2018. Dual antibacterial behavior of a curcumin-upconversion photodynamic nanosystem for efficient eradication of drug-resistant bacteria in a deep joint infection. J Mater Chem B 6, 7854–7861.

Lu, T., Ten Hagen, T.L.M., 2020. A novel kinetic model to describe the ultra-fast triggered release of thermosensitive liposomal drug delivery systems. J Control Release 324, 669–678.
Maldonado-Carmona, N., Ouk, T.S., Calvete, M.J.F., Pereira, M.M., Villandier, N., Leroy-Lhez, S., 2020. Conjugating biomaterials with photosensitizers: advances and perspectives for photodynamic antimicrobial chemotherapy. Photochem Photobiol Sci 19, 445–461.
Marini, E., Di Giulio, M., Magi, G., Di Lodovico, S., Cimarelli, M.E., Brenciani, A., Nostro, A., Cellini, L., Facinelli, B., 2018. Curcumin, an antibiotic resistance breaker against a multiresistant clinical isolate of Mycobacterium abscessus. Phytother Res 32, 488–495.
Moussa, Z., Chebl, M., Patra, D., 2017. Fluorescence of tautomeric forms of curcumin in different pH and biosurfactant rhamnolipids systems: Application towards on-off ratiometric fluorescence temperature sensing. Journal of Photochemistry and Photobiology B: Biology 173, 307–317.
Mun, S.H., Joung, D.K., Kim, Y.S., Kang, O.H., Kim, S.B., Seo, Y.S., Kim, Y.C., Lee, D.S., Shin, D.W., Kweon, K.T., Kwon, D.Y., 2013. Synergistic antibacterial effect of curcumin against methicillin-resistant Staphylococcus aureus. Phytomedicine 20, 714–718.
Naoum, S., Koutserimpas, C., Pantekidis, I., Giovanoulis, V., Veizi, E., Piagkou, M., Ioannou, P., Samonis, G., Domouchtsidou, A., Tsantes, A.G., Papadopoulos, D.V., 2024. Antimicrobial Regimens in Cement Spacers for Periprosthetic Joint Infections: A Critical Review. Antibiotics.
Partridge, S.R., Kwong, S.M., Firth, N., Jensen, S.O., 2018. Mobile Genetic Elements Associated with Antimicrobial Resistance. Clin Microbiol Rev 31.
Patra, D., Barakat, C., 2011. Synchronous fluorescence spectroscopic study of solvatochromic curcumin dye. Spectrochimica Acta Part A: Molecular and Biomolecular Spectroscopy 79, 1034–1041.
Pemmada, R., Shrivastava, A., Dash, M., Cui, K., Kumar, P., Ramakrishna, S., Zhou, Y., Thomas, V., Nanda, H.S., 2023. Science-based strategies of antibacterial coatings with bactericidal properties for biomedical and healthcare settings. Current Opinion in Biomedical Engineering 25, 100442.
Pitarresi, G., Palumbo, F.S., Calascibetta, F., Fiorica, C., Di Stefano, M., Giammona, G., 2013. Medicated hydrogels of hyaluronic acid derivatives for use in orthopedic field. Int J Pharm 449, 84–94.
Priyadarsini, K.I., 2009. Photophysics, photochemistry and photobiology of curcumin: Studies from organic solutions, bio-mimetics and living cells. Journal of Photochemistry and Photobiology C: Photochemistry Reviews 10, 81–95.
Pulla Reddy, A.C., Sudharshan, E., Appu Rao, A.G., Lokesh, B.R., 1999. Lipids 34, 1025–1029.
Racz, L.Z., Racz, C.P., Pop, L.-C., Tomoaia, G., Mocanu, A., Barbu, I., Sárközi, M., Roman, I., Avram, A., Tomoaia-Cotisel, M., Toma, V.-A., 2022. Strategies for Improving Bioavailability, Bioactivity, and Physical-Chemical Behavior of Curcumin. Molecules.
Romano, C.L., Malizos, K., Capuano, N., Mezzoprete, R., D'Arienzo, M., Van Der Straeten, C., Scarponi, S., Drago, L., 2016. Does an Antibiotic-Loaded Hydrogel Coating Reduce Early Post-Surgical Infection After Joint Arthroplasty? J Bone Jt Infect 1, 34–41.
Romano, C.L., Scarponi, S., Gallazzi, E., Romano, D., Drago, L., 2015. Antibacterial coating of implants in orthopaedics and trauma: a classification proposal in an evolving panorama. J Orthop Surg Res 10, 157.
Rubinstein, E., Keynan, Y., 2014. Vancomycin Revisited – 60 Years Later. Frontiers in Public Health 2.
Salehi, B., Stojanović-Radić, Z., Matejić, J., Sharifi-Rad, M., Anil Kumar, N.V., Martins, N., Sharifi-Rad, J., 2019. The therapeutic potential of curcumin: A review of clinical trials. European Journal of Medicinal Chemistry 163, 527–545.
Shome, S., Talukdar, A.D., Upadhyaya, H., 2022. Antibacterial activity of curcumin and its essential nanoformulations against some clinically important bacterial pathogens: A comprehensive review. Biotechnology and Applied Biochemistry 69, 2357–2386.
Sood, A., Dev, A., Das, S.S., Kim, H.J., Kumar, A., Thakur, V.K., Han, S.S., 2023. Curcumin-loaded alginate hydrogels for cancer therapy and wound healing applications: A review. Int J Biol Macromol 232, 123283.
Spichler-Moffarah, A., Rubin, L.E., Bernstein, J.A., O'Bryan, J., McDonald, E., Golden, M., 2023. Prosthetic Joint Infections of the Hip and Knee Among the Elderly: A Retrospective Study. Am J Med 136, 100–107.
Strimpakos, A.S., Sharma, R.A., 2008. Curcumin: preventive and therapeutic properties in laboratory studies and clinical trials. Antioxid Redox Signal 10, 511–545.
Tsuda, T., 2018. Curcumin as a functional food-derived factor: degradation products, metabolites, bioactivity, and future perspectives. Food & Function 9, 705–714.
Turner, A.B., Giraldo-Osorno, P.M., Douest, Y., Morales-Laverde, L.A., Bokinge, C.A., Asa'ad, F., Courtois, N., Palmquist, A., Trobos, M., 2025. Race for the surface between THP-1 macrophages and Staphylococcus aureus on various titanium implants with well-defined topography and wettability. Acta Biomaterialia 191, 113–139.
Uneputty, A., Dávila-Lezama, A., Garibo, D., Oknianska, A., Bogdanchikova, N., Hernández-Sánchez, J.F., Susarrey-Arce, A., 2022. Strategies applied to modify structured and smooth surfaces: A step closer to reduce bacterial adhesion and biofilm formation. Colloid and Interface Science Communications 46, 100560.
Virzi, N.F., Fallica, A.N., Romeo, G., Greish, K., Alghamdi, M.A., Patane, S., Mazzaglia, A., Shahid, M., Pittala, V., 2023. Curcumin I-SMA nanomicelles as promising therapeutic tool to tackle bacterial infections. RSC Adv 13, 31059–31066.
Yadav, S., Singh, A.K., Agrahari, A.K., Sharma, K., Singh, A.S., Gupta, M.K., Tiwari, V.K., Prakash, P., 2020. Making of water soluble curcumin to potentiate conventional antimicrobials by inducing apoptosis-like phenomena among drug-resistant bacteria. Scientific Reports 10, 14204.
Yin, W., Wang, Y., Liu, L., He, J., 2019. Biofilms: The Microbial "Protective Clothing" in Extreme Environments. Int J Mol Sci 20.
Zagami, R., Barattucci, A., Monsù Scolaro, L., Viale, M., Raffaini, G., Maria Bonaccorsi, P., Mazzaglia, A., 2023. Curcumin/amphiphilic cyclodextrin nanoassemblies: Theoretical and spectroscopic studies to address their debut in anticancer therapy. Journal of Molecular Liquids 389, 122841.
Zheng, D., Huang, C., Huang, H., Zhao, Y., Khan, M.R.U., Zhao, H., Huang, L., 2020. Antibacterial Mechanism of Curcumin: A Review. Chem Biodivers 17, e2000171.